Proceedings of 20th International Congress on Acoustics, ICA 2010

23-27 August 2010, Sydney, Australia

Liquid Mixing using Streaming in Frequency-Modulated Ultrasound Beams Radiated from SAW Devices

Miyuki Maezawa (1), Hideyuki Nomura (2) and Tomoo Kamakura (2)

(1) Olympus, 2-3 Kuboyama-cho, Hachioji-shi, Tokyo 192-8512, Japan
(2) The University of Electro-Communications, 1-5-1 Chofugaoka, Chofu-shi, Tokyo 182-8585, Japan

PACS: 43.25.Nm, 43.35.Pt

ABSTRACT

This report presents a promising investigation on liquid mixing using streaming in ultrasound beams that are generated by interdigital transducers on an 128◦ X-cut Y-propagation $LiNbO_3$ substrate in frequency-modulated signals. The device radiates two beams in a liquid in the directions that are determined by the Rayleigh angle and Snell's law. The simplified theory that predicts the frequency-dependent profiles of the beam is supported by the appropriate measurement of sound pressure fields. Optimum sweep driving in frequency-modulation improves liquid mixing efficiently. This method makes it possible to change the flow field temporally and spatially by only a single IDT device. Mixing efficiency as well as miniaturization of devices can be then achieved successfully.

INTRODUCTION

Recently, much attention has been paid to handling technologies in microfluidics. Miniaturization of chemical devices, for example, in mixing and separation processes, is needed under environmental awareness including energy saving, compact size, and safety aspects.

For a liquid in micro-scaled volume, interface interaction between the fluid and the walls of a container becomes dominant in mixing. Additionally, the Reynolds number is so small that it is not easy to mix different fluids by turbulent flow in a short amount of time. As a promising technique for realizing effective mixing in such microfluidic systems, acoustic streaming generated by surface acoustic waves (SAWs) has been given attention [1], [2]. It has been experimentally demonstrated that the streaming using SAW can achieve mixing dramatically in a very short time by radiating ultrasound beams in a liquid obliquely [3]. Interestingly, SAW devices using plural interdigital transducers (IDTs) have advanced performance in mixing due to the spatial and temporal generation of chaotic flow [4], [5]. One of the authors has reported that a wave mode method utilizing both SAWs and bulk acoustic waves (BAWs) generated from the IDTs on a Y-cut Z-propagation $LiNbO_3$ substrate can achieve the improvement of mixing performance because of chaotic flow and miniaturization [6]. Unfortunately, the energetic efficiency of a Y-Z $LiNbO_3$ substrate has no advantage over an 128◦ Y-cut X-propagation $LiNbO_3$ substrate [7]. Additionally, 128◦ Y-X $LiNbO_3$ substrates radiate two beams in water [8], and the one radiation angle of those is frequency-dependent [9]. This paper proposes another method that successfully uses a SAW device with an 128◦ Y-cut X-propagation $LiNbO_3$ substrate by means of frequency-modulation (FM) technique for improving mixing efficiency. Since acoustic streaming depends strongly on ultrasound pressure fields, the spatial profiles of the beam emitted from the IDT device are measured in water using a miniature hydrophone with a small sensitive area. Flow fields that play an important role in liquid mixing are visualized by particle image velocimetry (PIV) system. Furthermore, the effectiveness of frequency-modulated driving is evaluated by measuring mixing time of different kinds of liquids in several µl.

FLOW CONTROL BY FM DRIVING

Basic principle

Figure 1 shows an IDT configuration we are concerned with in this report. Here, h, a and $l = a + h$ are the line width, space width and electrode period, respectively. SAW is excited most strongly when its wavelength λ_s equals to $2l$. At this excitation, the following relationship between the frequency f_s and the propagation speed vs of the Rayleigh wave on the device holds:

$$f_s = \frac{v_s}{2l} = \frac{v_s}{2(a+h)} \tag{1}$$

When IDTs are excited in water, SAWs are converted into longitudinal waves that propagate in water as ultrasound beams in the directions determined by the Rayleigh angle θ_R. The angle that obeys Snell's law is reduced to be the ratio of the propagation speed v_0 in water to the propagation speed v_s [10]:

$$\theta_R = \sin^{-1}\left(\frac{v_0}{v_s}\right) \tag{2}$$

Since v_0 in water is 1500 m/s and v_s on a 128◦ Y-cut X-propagation $LiNbO_3$ substrate is v_s = 3960 m/s, the Rayleigh angle θ_R takes a value of 22.3◦. Hence two ultrasound beams propagate in water along the different axes with $\pm\theta_s$ (= 90◦ - θ_R). In addition to the SAWs, the longitudinal waves that spread cylindrically from a pair of IDTs as a wave source of

the delta function are strongly propagated as well into the directions of $\pm\theta_d$. The angle θ_d is determined by the following formula [9]:

$$\theta_d = \cos^{-1}\left(\frac{2\pi / d}{\omega / v_0}\right) = \cos^{-1}\left(\frac{v_0}{f \cdot d}\right) \quad (3)$$

where, f is the driving frequency, and $d = 2l$. From this formula, the more the driving frequency increases the smaller the angle θ_d becomes, under otherwise unchanged conditions. We can therefore expect that the radiation angle of ultrasound beams and the consequent flow angle of acoustic streaming vary with the driving frequency. It enables us to control the flow field accordingly.

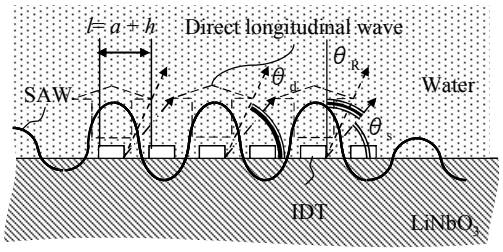

Figure 1. Illustration diagram of an IDT and its mode conversion at the interface. Propagation of sound waves is depicted in one side only as arrows for brevity. (a) The radiation angle of longitudinal wave converted from SAWs is θ_s . (b) The radiation angle of longitudinal wave generated directly by the IDT is θ_d.

Experimental verification

To confirm the effectiveness of the theory developed above, we measure both sound field and flow field using a SAW device with a center frequency of 20 MHz. The SAW device used consists of 25 pairs of 2-mm aperture IDT electrodes at electrode period of 99 μm with a center frequency of 19.6 MHz [11]. The device is mounted on the inner wall of a tank whose sizes are 240 × 300 × 180 mm^3 and is filled with pure water. The water temperature is kept to be around 26 ºC.

Ultrasound field measurement

The block diagram of the experimental setup for ultrasound field measurement is shown in Fig. 2. Tone-burst signals with 20 cycles at frequencies of 17.6, 19.6($= f_s$) and 21.6 MHz are generated by a function generator (Agilent, 33250A) are fed through a power amplifier (Kalmus, 150C) to the SAW device with a 50 Ω matching circuit. The input electric power to the device is 0.5 W, which is monitored by a power meter (Diamond SX-200).

One of the two ultrasound beams radiated in water at the angles of $\pm\theta$ from the SAW device is detected using a miniature hydrophone (Onda, HNP-0400) that has an element diameter of 0.4 mm, and is calibrated over a wide frequency range from 1 to 40 MHz. The hydrophone is mounted on a positioning system (x-y-z stage) that can move it precisely with the translation sliders. All the movements in the longitudinal (z'), horizontal (x'), and vertical (y) directions are controlled by a personal computer. Ultrasound pressure signals were transmitted to a digital storage oscilloscope (LeCroy, 9310C) with a built-in Fast Fourier transform (FFT) analyzer. It is well-known that harmonic generation in ultrasound beams due to the nonlinearity of medium results in extra dissipation of the sound energy and enhances the driving force of acoustic streaming. We then measure not only the fundamental but also second harmonic sound pressure amplitudes. These measured data are stored in the memory of the personal computer via a GPIB cable. 100 times of averaging are performed at every hydrophone's position to improve SN ratio.

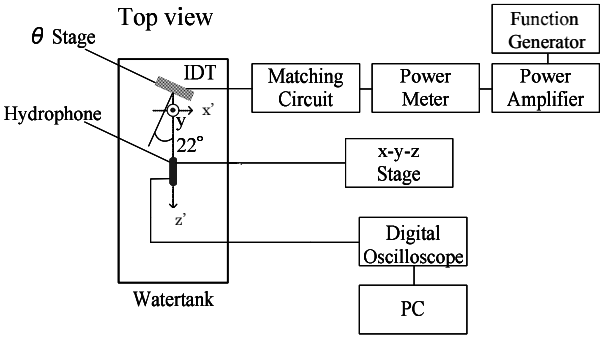

Figure 2. Experimental setup for measurement of sound field.

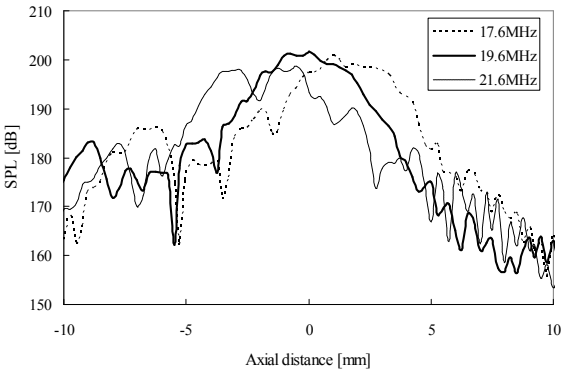

Figure 3. Beam patterns of the fundamental pressure amplitudes at 45 mm from the SAW device.

Measured beam patterns at a distance of 45 mm from the device are shown in Fig. 3 when the hydrophone is moved along the x' axis from −10 mm to 10 mm. As can be seen, the beam profiles vary with driving frequency apparently. Especially, the peak position of sound pressure moves more inside when the frequency is increased.

Figures 4 and 5 show the experimental data of the fundamental and second harmonic pressure distributions on the $x' - z'$ plane, respectively. We can confirm that both the pressure beams move in the negative direction along x'-axis. For example, the fundamental frequency beam at 21.6 MHz moves by 4 mm at $z' = 90$ mm compared with the beam at 19.6 MHz. This moving distance corresponds to the increase of the beam angle $\theta = \theta_d - \theta_s$ by $\tan^{-1}$ (4 mm / 90 mm) ≈ 2.5◦. The similar decrease of the beam angle is seen in the second harmonic pressure data.

Interestingly, the contrast of the second harmonic beams is higher and the boundary outline of the beam is clearer than those of the fundamental beams. Additionally, the beamwidth of the second harmonic is approximately equal to the aperture size of the IDTs. However, the pressure levels of the harmonic are generally 15-dB lower than those of the fundamental.

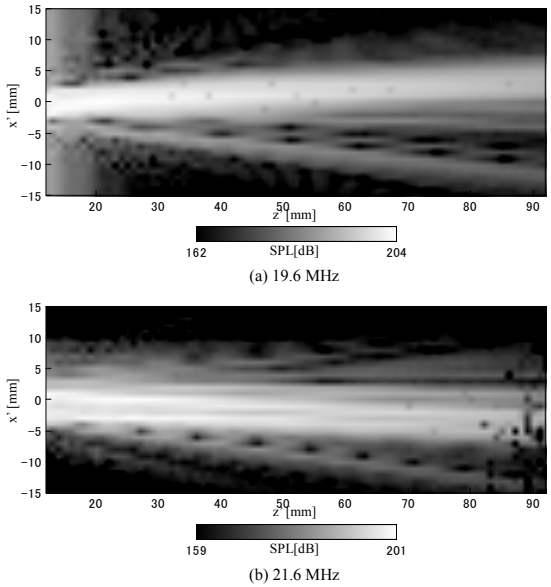

Figure 4. Pressure distributions of the fundamental pressures in $x' - z'$ plane using the 25-pair IDTs driven at (a) 19.6 MHz, (b) 21.6 MHz.

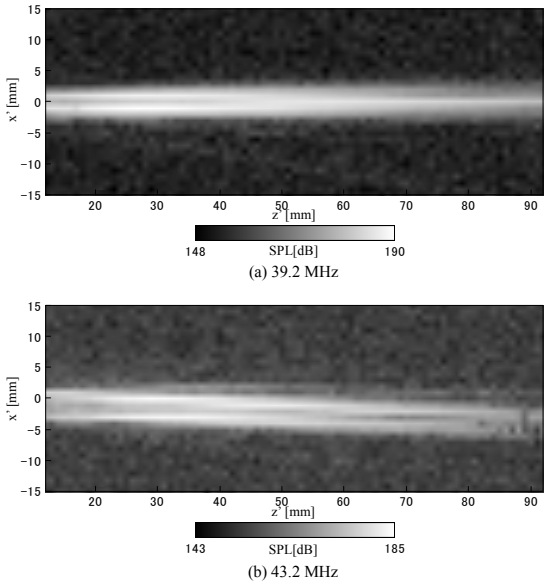

Figure 5. Pressure distributions of the second harmonic pressures in $x' - z'$ plane by the 25-pair IDTs driven at (a) 39.2 MHz, (b)43.2 MHz.

Since the driving force of the streaming is roughly proportional to the pressure amplitude squared, the contribution of the second harmonic beam on the driving force is probably of the order of ten percent.

Now compare the experimental results with theoretical predictions in detail. The resonance frequency is theoretically predicted to be 20 MHz from the electrode period pitch l = 99 μm and SAW propagation speed v_s = 3960 m/s employing eq. (1), being only 0.4 MHz-higher than the experimental frequency of 19.6 MHz. Then, the radiation angle θ_s of the longitudinal wave into water is estimated as ± 67.7º from eq. (2). When the theoretical driving frequency is 22 MHz that corresponds to the experimental frequency of 21.6 MHz, the radiation angle θ_d takes a value of 69.9º by eq. (3). This means that the theoretical beam with the driving frequency 21.6 MHz moves inside by 2.1º compared with the angle at the center frequency (20 MHz). We note that the theoretical moving angle θ of 2.1º agrees well with the experimental result of 2.5º.

Flow field visualization

Acoustic streaming from the IDT-side of the device at 0.5 W is visualized by particle image velocimetry (PIV). The experimental setup for flow field measurement is almost the same as the previous report [6]. In this study, flows are measured at driving frequencies of 17.8 MHz, 19.6 MHz (center frequency) and 21.8 MHz. Monochromatic CW from a function generator is power-amplified to drive the IDT device at 0.5 W.

Flow fields visualized by the PIV system are shown in Fig. 6. In the same way as the ultrasound beams, the angle of the streaming is decreased when the driving frequency is increased. The flow at the center frequency (19.6 MHz) is almost symmetry with respect to the z-axis and the flow velocity near the device is the fastest. By contrast, the velocity at 21.8 MHz is the slowest of the three frequency conditions. Such velocity-reduction is probably attributed to the reason that driving the SAW device at frequencies much different from the center frequency increases the loss of effective power because of impedance mismatch.

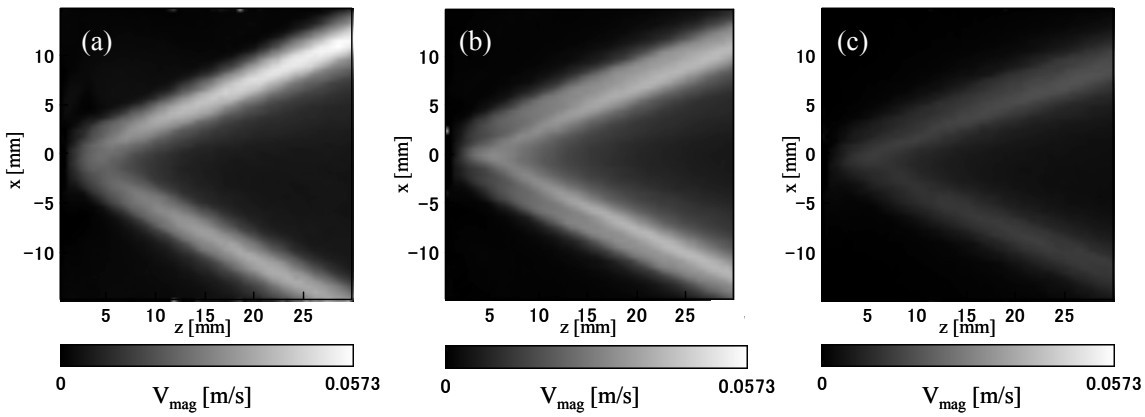

Figure 6. Flow fields of streaming by driving at 17.8 MHz (a), 19.6 MHz (b) and 21.8 MHz (c).

LIQUID MIXING BY FREQUENCY-MODULATED SIGNAL

Experimental methodology

In the preceding chapter, we observed that driving frequency changes spatially both sound beam and flow profiles. Now we apply this experimental finding to the effective mixing of liquids by driving a SAW device in frequency-modulated signals. Generally, ultrasound beams at higher frequencies increase the driving force acting on the fluid and enhance acoustic streaming. Consequently, quick mixing of microfluidics may be realized. We then make use of a SAW device that operates at a frequency of about 100 MHz to enhance acoustic streaming in a microcell.

The experimental setup is shown in Fig. 7. We prepare for a reaction cell whose opening area is 2 mm by 3 mm with 0.5-mm corners at its intersections and is made of polystyrene. The device consists of 19 pairs of 2.15-mm- aperture IDT electrodes with the center frequency of 98 MHz on an 128◦ Y-cut X-propagation $LiNbO_3$, and is placed just under the cell so as to meet the bottom center of the reaction cell after water as an acoustic propagation medium is delivered on the IDT. The electric signal of 0.5 W is fed via a power-amplifier to the device.

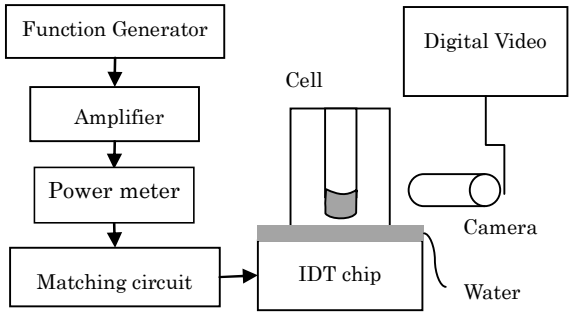

Figure 7. Experimental setup of liquid mixing.

The procedure of fluid mixing by streaming is as follows. First, funnel polyvinyl alcohol (PVA) solution of 7 µl into the cell. Next, funnel gently Evans Blue solution of 1 µl into the same cell. The viscosities of the two solutions are the same to be 3 mPa·s. Driving signals are input to the device after a video camera starts shooting. We evaluate the mixing time of liquids as elapsed time from T_1 to T_2 ; i.e., $T_2 - T_1$, where T_1 is the beginning time of signal driving and T_2 is the ending time at which brightness in shot images does not change.

Behavior of acoustic streaming versus driving frequency

A sample of liquid flow in the reaction cell is shown in Fig. 8. In this picture, solid arrows in white show the direction of the streaming and four dotted lines indicate vortexes. Figure 9 shows the source points by two arrows at different driving frequencies; i.e., (a) at 96 MHz, (b) at 104 MHz. It should be noted that the higher the driving frequency is the narrower the distance between the two source points becomes. Insofar as the driving frequency does not change, the vortexes remain still separated. If the driving condition is continuously changed from (a) to (b) or vice versa in Fig. 9, for example, the interfusion of four vortexes can be expected. We introduce therefore an alternative method that uses frequency-modulated signals for realizing effective mixing.

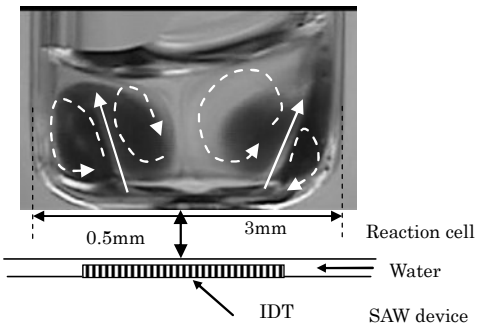

Figure 8. Liquid flow in a cell during mixing.

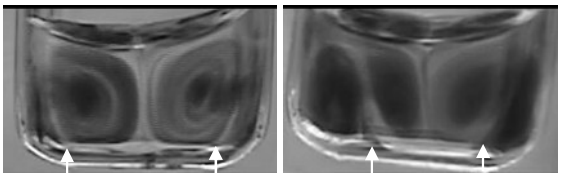

Figure 9. Liquid flows in a cell during mixing at 96 MHz (a) and 104 MHz (b).

Effect of frequency modulation in mixing

Figure 10 shows the impedance characteristic of the device, in which solid and dotted lines denote the magnitude and phase, respectively. In the same figure the measured data of mixing time are shown in filled circles as a function of driving frequency. In this experimental situation the driving signal is not modulated. We can observe from these data that the mixing efficiency becomes the highest when the phase is closer to zero. This means that driving is operated near 98 MHz, i.e., the center frequency of the SAW. The shortest mixing time of 15 sec is realized at this frequency.

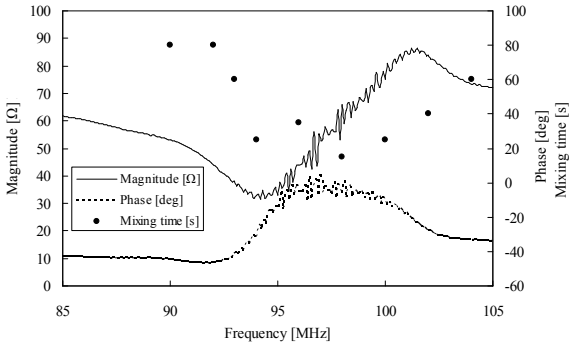

Figure 10. Impedance characteristic and relations of mixing time vs. driving frequency.

Figure 11 shows the relationship between mixing time and sweep time when the driving frequency is modulated with a frequency deviation of 10 MHz from 98 MHz. The mixing time at the sweep time of 0.33 sec becomes half when the device is driven monochromatically at 98 MHz. Insofar as the sweep time is set between 0.1 to 1 sec, the mixing perform-

ance changes slightly. The performance decreases functionally when the sweep time is set under 0.1 sec or above 1 sec.

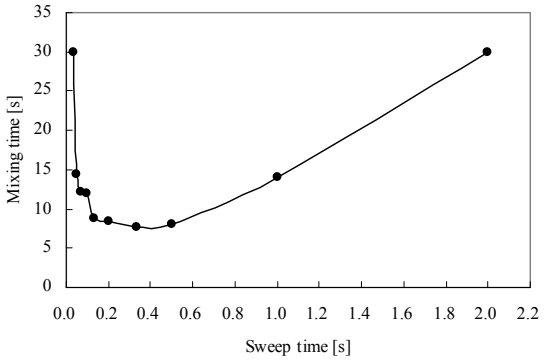

Figure 11. Mixing time vs. sweep time of FM driving signal.

Figure 12 shows the mixing time as a function of frequency deviation. Source signals are monochromatic waves of the center frequency 98 MHz and sweep time 0.33 sec. The sweep frequencies are changed from 1 to 10 MHz. It is apparent from this figure that mixing performance is effective in sweeping the signal from 3 to 5 MHz. The performance is not successful when the frequency deviation is too small or too large. When the frequency deviation is small, chaotic flows hardly occur because the flow patterns do not change greatly. Whereas, flow velocities themselves get slow when the frequency deviation is too large. This slowness in velocity is ineffective in mixing.

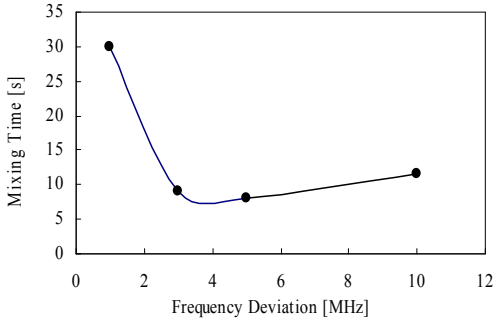

Figure 12. Mixing time vs. sweep frequency of FM driving signal.

CONCLUSIONS

Frequency-modulated signals in driving SAW devices can change spatial profiles of ultrasound pressure amplitudes and flow patterns as well. The thus obtained changing in flow profiles have demonstrated that an optimized sweep frequency can improve effectively the performance of mixing using an 128◦ Y-cut X-propagation mode of $LiNbO_3$. This is expected to be a promising method for realizing chaotic mixing in microfluidic technology. In this preliminary study, efficient mixing has been observed using only a fluid in a cell. Since the generation of acoustic streaming depends on not only driving frequency but also viscosity of fluids, the optimal conditions for mixing should be determined by taking account of the fluid volume and cell configuration. In such an involved situation, computational fluid dynamics (CFD) may be a useful tool for numerically predict the optimal efficiency in mixing.

REFERENCES

1 K. Sritharan, C. J. Strobl, M. F. Schneider, A. Wixforth, and Z. Guttenberg, “Acoustic mixing at low Reynold’s numbers” , *Appl. Phys. Lett*. **88**, 054102 (2006).

2 E. Galopin, A. Renaudin, J. C. Camart, V. Thomy, C. Druon, and P. Tabourier: “Enhanced Protein Capture By Ultrafast SAW Droplet μMixing”, *Proc. International Conference on Miniaturized Systems for Chemistry and Life Sciences (μTAS2006)*, No. 10, 651-653, Tokyo, Japan (2006-11).

3 A. Rathgeber, M. Wassermeier and A. Wixforth, “Acoustic ‘distributed source’ mixing of smallest fluid volumes”, *J. of ASTM Interna*. **2**, **6** (2005).

4 W. Tseng, J. Lin, W. Sung, S. Chen, and G. Lee, “Active micro-mixers using surface acoustic waves on Y-cut 128◦ $LiNbO_3$”, *J. Micromech. Microeng.*, **16**, 539-548, (2006).

5 T. Frommelt, M. Kostur, M. Wenzel-Schäfer, P. Talkner, P. Hänggi, and A. Wixforth, “Microfluidic mixing via acoustically driven chaotic advection”, *Phys. Rev. Lett.* **100**, 034502 (2008).

6 M. Maezawa, T. Kamakura, K. Matsuda, “Generation and Visualization of Acoustic Streaming by Bulk Acoustic Waves from Interdigital Transducers”, *Trans. IEICE,* **J91-A**, **12**, 1-8 (2008) [in Japanese].

7 T. Moriizumi, T. Nakamoto and T. Kikuchi, “Selection of Piezoelectric Materials used for Interdigital Transducer in Water”, *Trans. IECE*, **J65-A**, **5**, 489-490 (1982) [in Japanese].

8 K. Kobayashi, T. Moriizumi and K. Toda, “Longitudinal acoustic wave radiated from an arched interdigital transducer”, *J. Appl. Phys*., **52**, **8**, 5386-5388 (1981).

9 T. Moriizumi, T. Kikuchi, T. Nomura, T. Yasuda and K. Toda, “Study on IDT for Acoustic Imaging Uses”, *IECE*, **J65-A**, **7**, 611-618 (1982) [in Japanese].

10 S. Shiokawa, Y. Matsui and T. Moriizumi, “Experimental Study on Liquid Streaming by SAW”, *Jpn. J. Appl. Phys*. **28**, Suppl. 28-1, 126-128 (1989).

11 M. Maezawa, R. Kamada, T. Kamakura, and K. Matsuda, “Nonlinear Sound Field by Interdigital Transducers in Water ”, *Jpn. J. Appl. Phys*., **47 (5B)**, 4076-4080 (2008).